

From microns to kissing contact: Dynamic positioning of two nano-systems

Kevin J. Savage,^{a)} Matthew M. Hawkeye, Bruno F. Soares, and Jeremy J. Baumberg^{b)}
Cavendish Laboratory, University of Cambridge, Cambridge CB3 0HE, United Kingdom

(Received 11 May 2011; accepted 16 July 2011; published online 3 August 2011)

Two conducting atomic force microscopy probes are brought into three-dimensional nanoscale “tip-to-tip” alignment with dynamically controlled spacing and ultra-wide optical access. We utilize resonant electrical parametric mixing, created by the electromechanically coupled tips, to extract the electronic signal due to nanoscale changes in inter-tip position. Experimental results match theory confirming the viability of the technique. By functionalizing the tip apices, this advanced multi-functional observation platform allows simultaneous measurement of the optical and electronic response of nanoparticle dimers, at sub-nanometer separations. © 2011 American Institute of Physics. [doi:10.1063/1.3623437]

Understanding the simultaneous optical and electronic response of nanoparticle (NP) systems at sub-nanometer separation is currently of great interest.¹ Such metallic nano-systems introduce quantum phenomena into non-linear and active plasmonics, and surface enhanced- and THz-spectroscopies. Extreme field enhancements, and shifted or split plasmonic modes, are vital for a large range of applications.^{1,2} Thus investigations of the atomic scale transition from an electrically separated to a conductively linked NP dimer are of fundamental importance. Unfortunately, optically accessible NP dimers with variable separation are challenging to create experimentally. Current methods include directed self-assembly,^{3,4} top-down lithography,⁵ and discrete-step nanomechanical manipulation.⁶ Recent self-assembly methods enable spectroscopy on NP dimers of fixed separations down to approximately 0.7 nm.⁷ However, none of these techniques provide dynamic control of dimer alignment and separation, limiting their capability for optical investigations of NP dimer interactions at the quantum scale. These techniques also lack the capability for simultaneous measurement of individual NP dimer optical and electronic response.

In the field of molecular electronics, conductive contact to molecular junctions for simultaneous dynamic optical and electronic measurement has been achieved using electromigration⁸ and mechanically controllable break-junction (MCBJ) methods.⁹ The use of MCBJ techniques provides the stability required to create long-lived molecular scale junctions. However, the techniques lack the dynamic range of alignment, separation, NP geometry, and control of contact required to investigate the full range of plasmonic response.

In this letter, we report a compact approach for creating an *optically accessible* NP dimer with *dynamically* controllable separation from over 500 nm to full conductive contact, without the need for top-down processing or the limited access of a commercial atomic force microscope (AFM). The technique is based on the three-dimensional (3D) nanoscale alignment of two conducting AFM probes in a “tip-to-tip” configuration. A NP can be created on the apex of each

probe by a wide variety of methods including, metallic coating,¹⁰ mechanically directed or chemically based NP attachment,¹¹ and by focused ion beam milling.¹² To achieve a large dynamic range of alignment, our electrostatic force microscopy technique uses an alternating potential applied across the conducting AFM tips to create an oscillating long-range electrostatic force. We exploit the non-linear electrical parametric response of the electromechanically coupled tip system to align the NP dimer with nanometer-scale precision.

The experimental setup and coordinate system used for modeling are shown in Fig. 1. The frequency range of interest is around the fundamental flexural mode of the cantilevers and therefore the tip system is modeled as a pair of coupled point-mass harmonic oscillators. The tips are coupled through the superposition of the z -components of the driving electrostatic attractive force F_{EL}^z and the short-range (<2 nm) Van der Waals and repulsive tip-tip interaction forces F_{TT}^z . The coupled equations of motion for tips $i=(1,2)$ with apex positions z_i and apex separation $d(t) = z_1(t) - z_2(t)$ are

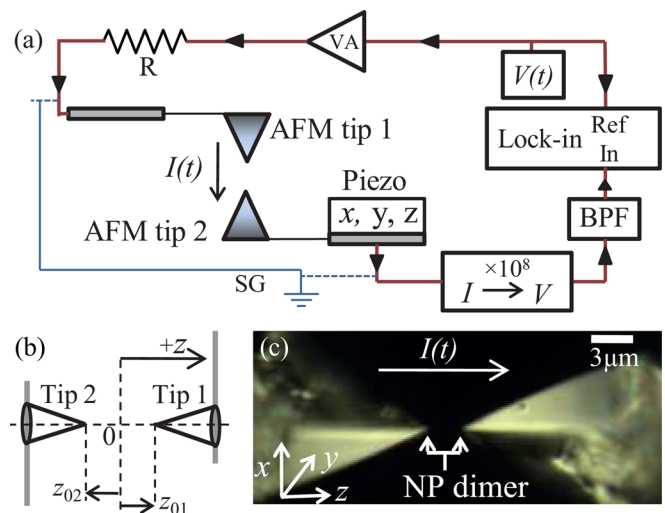


FIG. 1. (Color online) (a) Experimental setup with signal ground (SG), BPF, and voltage amplifier (VA). (b) Coordinate system used in theoretical analysis. (c) Dark-field image of metal coated AFM tips.

^{a)}Electronic mail: kjs61@cam.ac.uk.

^{b)}Electronic mail: jjb12@cam.ac.uk.

$$m_i \frac{d^2 z_i}{dt^2} + \beta_i^z \frac{dz_i}{dt} + k_i^z (z_i - z_{0i}) = \pm (F_{EL}^z + F_{TT}^z), \quad (1)$$

where m_i is the effective mass, $\beta_i^z = \beta_{0i}^z + \beta_{TT}^z$ is the z -component of the non-linear damping coefficient, $k_i^z = k_{0i}^z + k_{TT}^z$ is the z -component of the cantilever spring constant, and z_{0i} is the tip apex position when $F_{EL}^z = F_{TT}^z = 0$. The sign of the RHS force term is positive for tip 1 and negative for tip 2. For comparison with experiment, Eq. (1) is solved numerically using a standard fifth-order Runge-Kutta algorithm. Tip parameters m_i and β_{0i}^z are derived from k_{0i}^z and experimentally measured values of the appropriate cantilever resonance frequencies ω_{0i} and Q-factors Q_{0i} . Using the approximations implemented in Ref. 13 for an axially symmetric AFM tip, analytical expressions for F_{EL}^z and capacitance (C) are derived for two identical cones in a tip-to-tip geometry. The associated cantilevers are treated as a parallel-plate capacitor. These expressions are valid for all values of d considered and are functions of cone height, apex radius (R_i), cone angle, and cantilever overlap area (A^{ov}). The position dependent damping and spring constant terms β_{TT}^z and k_{TT}^z were modeled by the air “squeeze” damping between two parallel plates of area chosen by experimental fit.¹⁴ The short-range interaction F_{TT}^z is treated as a Lennard-Jones force of the form¹⁵ $F_{TT}^z = F_{VdW}^z + H\bar{R}a_0^6/180d^8$, where H is the material-dependent Hamaker constant, $\bar{R} = R_1R_2/(R_1 + R_2)$ is the reduced apex radius, a_0 is the material dependent interatomic distance, and F_{VdW}^z is the attractive Van der Waals force between the two cones estimated from Ref. 16. Alignment is implemented in the non-contact regime hence contact dynamics, such as adhesion forces and surface deformation are not treated. The surrounding support structure is modeled by a relatively large constant stray capacitance ($C_{bk} \approx 0.1$ pF) in parallel with the dual tip-cantilever capacitor. The current flow through the system is calculated and the magnitude and phase of the harmonic components determined by subsequent Fourier analysis.

To allow a simpler analytical analysis, we approximate the tips as a parallel plate capacitor in the long-range regime ($F_{TT}^z = \beta_{TT}^z = k_{TT}^z = 0$). The force due to the capacitance is given by

$$F_{EL}^z(V, d) = \frac{1}{2} \frac{\partial C}{\partial d} V^2(t), \quad (2)$$

where $V(t)$ is the applied potential. By applying $V(t) = V_0 \cos(\omega_s t)$ at a signal frequency $\omega_s \approx \omega_{01}/2$, Eq. (2) shows that F_{EL}^z and hence $C(t)$ will primarily oscillate resonantly at $\omega_p = 2\omega_s \approx \omega_{01}$, where ω_p is the pump frequency. Driving at $\omega_{01}/2$ allows only the direct ω_{01} resonance of the tip system to be efficiently excited rather than the mechanical parametric resonance at $2\omega_{01}$. This is critical to avoid driving the tip system response into a parametric instability domain.¹⁷ Assuming $z_{02} = 0$ and tip 2 is stationary, the tip apex separation at zero applied force $d_0 = z_{01} - z_{02}$ is equal to z_{01} and Eq. (1) reduces to a single equation of motion

$$m_1 \frac{d^2 z_1}{dt^2} + \beta_{01}^z \frac{dz_1}{dt} + k_{01}^z (z_1 - d_0) = F_{EL}^z(z_1, t). \quad (3)$$

Solving Eq. (3) in the limit of small tip oscillations $|\Delta z_1| \ll d_0$ gives $z_1(t)$. Using $C = (\epsilon_0 A^{ov}/z_1) + C_{bk}$ and $I = C(dV/dt)$

+ $V(dC/dt)$ yields the associated first-order current flow, with Fourier coefficient magnitudes

$$|I(\omega_s)| \approx \omega_s C_0 V_0 \left\{ 1 + \frac{z_{off}}{d_0} + \frac{(\omega_p - \omega_s)|\Delta z_1|}{2d_0\omega_s} + \frac{C_{bk}}{C_0} \right\}, \quad (4a)$$

$$|I(\omega_p + \omega_s)| \approx \frac{(\omega_p + \omega_s)C_0 V_0 |\Delta z_1|}{2d_0}, \quad (4b)$$

where $C_0 = \epsilon_0 A^{ov}/d_0$ and z_{off} is the additional offset in tip position because $F_{EL}^z \propto V^2$. The oscillating non-linear tip capacitance at ω_p produces electric parametric mixing. This results in power transfer from the fundamental to sum and difference frequency components that are dependent on $|\Delta z_1|$. The current component at $\omega_p + \omega_s = 3\omega_s$ provides a background-free signal directly related to the magnitude and phase of the tip oscillation. The current component at $\omega_p - \omega_s = \omega_s$ creates the third term on the RHS of Eq. (4a). If tip 2 is scanned in the x or y directions, F_{EL}^z decreases along with C and hence $|\Delta z_1|$ is modified.¹⁸ This allows the tips to be precisely aligned in 3D by tracking the lock-in detected current at $3\omega_s$.

The tip system (Fig. 1(a)) is driven by an amplified signal generator and the current flow across the tips passed through a 10^8 gain transimpedance amplifier. A band-pass filter (BPF) centered at $3\omega_s$ prevents the current component at ω_s overloading the lock-in. The entire setup is placed on an active anti-vibration platform and contained within a Faraday cage. The tips are initially aligned to within ± 400 nm in x , y , z under a colinear custom-built microscope with $\times 100$, NA = 0.9 objective. The tips used here are 50 nm Au coated nano-indentation AFM probes with a “neck and ball” apex geometry. The tip system resonance behavior is characterized by performing a frequency sweep whilst measuring $|I(3\omega_s)|$. A typical response curve around half the resonance frequency of tip 1 (f_{01}) is shown in Fig. 2. The Fano-like lineshape measured is significantly different to the expected Lorentzian lineshape. This is due to interference between $I(3\omega_s)$ and the background signal I_{HD} created by the harmonic distortion (HD) of the electronic amplifiers. This HD was characterized and added to the theory via a $3\omega_s$ term in V , thus recovering the correct resonance lineshape. The

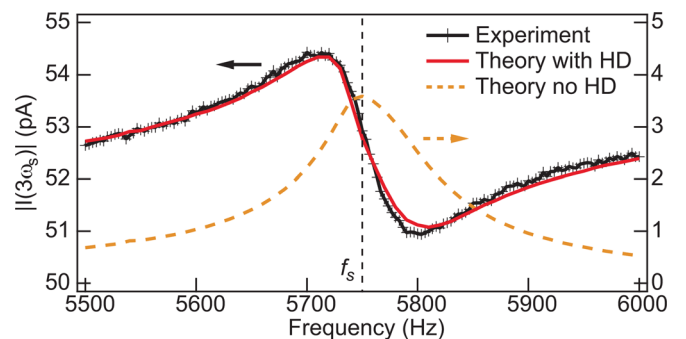


FIG. 2. (Color online) Measured $|I(3\omega_s)|$ (solid markers) vs. numerical simulation with the same parameters and HD included (solid line) and absent (dashed line). The frequency used for alignment scans is f_s .

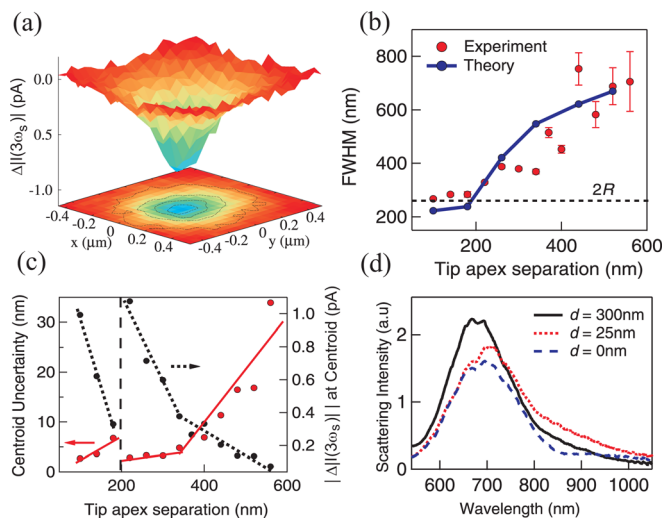


FIG. 3. (Color online) (a) Change in $|I(3\omega_s)|$ with respect to HD background vs. position of tip 2 in a $1 \times 1 \mu\text{m}^2$ grid with $d_0 = 260\text{ nm}$. (b) FWHM of $\Delta|I(3\omega_s)|$ minimum vs. tip-apex separation. (c) Uncertainty and magnitude associated with $\Delta|I(3\omega_s)|$ centroid vs. tip apex separation. Solid and dotted lines guide the eye, dashed vertical line shows $V_0 \rightarrow 0.78V_0$. (d) Dark-field spectra taken at $d_0 = 300\text{ nm}$ (solid line), 25 nm (dotted line), and 0 nm (dashed line).

resonant frequency of tip 1 is observed and the tips then driven at the frequency that maximizes sensitivity $f_s = f_{01}/2 = 5.75\text{ kHz}$.

For alignment, tip 2 is scanned over a $1 \times 1 \mu\text{m}^2$ grid whilst measuring $|I(3\omega_s)|$ at each position. Tip apex separation d_0 is reduced along with V_0 to prevent “snap to contact” phenomena and successive alignment scans are taken. A typical alignment scan showing the change in signal with respect to the HD background ($\Delta|I(3\omega_s)| = |I(3\omega_s)| - |I_{HD}|$) is shown in Fig. 3(a). The local minimum observed is again due to the interference between the $I(3\omega_s)$ and I_{HD} signals. As the tips approach, the magnitude of the signal minimum increases while the associated FWHM and the uncertainty in centroid location decrease (Figs. 3(b) and 3(c)). By thus “homing-in” on the centroid position to $d_0 < R_i \approx 130\text{ nm}$, the FWHM tends to $2R$ as expected. The numerical simulation FWHM results are in good agreement with experiment. This is expected as the required corrections in C and F_{EL}^z due to the tips moving off-axis are approximated to be $<15\%$. When $d_0 < R$, we set $V_0 = 0$ and d_0 is further reduced with nanometer precision using the piezoelectric actuator. An absolute distance scale is obtained by applying a small ($<30\text{ mV}$) stationary potential across the tips and controllably reducing d_0 whilst observing the current rise upon (mechanically reversible) atomic-scale kissing contact.

After alignment and distance calibration, dark-field scattering spectra are taken at different d_0 using a supercontinuum laser sourced confocal nano-spectroscopy setup. Spectra taken at the tip apexes in the plasmonic non-interacting, interacting,

and contact regimes are shown in Fig. 3(d). The incident light is polarized along the dimer axis hence decreasing d_0 increases the near-field dipole-dipole coupling that red-shifts the spectral response.⁷ Upon conductive contact, the dipole-dipole interaction is “shorted” and the spectra blue-shifts as competition begins between higher order modes (to be investigated elsewhere).

In conclusion, the parametric response of an electromechanically coupled AFM tip system is utilized as a long-range sensor of 3D tip-tip alignment. We experimentally and theoretically demonstrate this advanced technique for dynamic separation control of metallic NP dimers on the nanoscale. At all separations, the system maintains the facility for simultaneous local optical and electronic measurement. This enables a versatile experimental setup to perform time-resolved (μs) dark-field nano-spectroscopy in different plasmonic interaction regimes. By simultaneously measuring the optical response and electrical conductivity at $d_0 < 1\text{ nm}$, we aim to investigate the relationship between electronic quantum transport and the plasmon mediated response of metallic NP dimers. We expect techniques developed here will also find use in nonlinear and active plasmonics, surface enhanced spectroscopies, and THz quantum transport research.

The authors acknowledge Nanotools GmbH for providing the modified ball AFM tips and support from the UK EPSRC under Grant Nos. EP/G060649/1 and EP/F059396/1.

- ¹N. J. Halas, *Nano Lett.* **10**, 3816 (2010).
- ²J. A. Schuller, E. S. Barnard, W. Cai, Y. Jun, J. S. White, and M. L. Brongersma, *Nature Mater.* **9**, 193 (2010).
- ³S. K. Ghosh and T. Pal, *Chem. Rev.* **107**, 4797 (2007).
- ⁴L. Yang, H. Wang, B. Yan, and B. M. Reinhard, *J. Phys. Chem. C* **114**, 4901 (2010).
- ⁵S. S. Aćimović, M. P. Kreuzer, M. U. González, and R. Quidant, *ACS Nano* **3**, 1231 (2009).
- ⁶J. Merlein, M. Kahl, A. Zuschlag, A. Sell, A. Halm, J. Boneberg, P. Leiderer, A. Leitenstorfer, and R. Bratschitsch, *Nature Photon.* **2**, 230 (2008).
- ⁷S. Marhaba, G. Bachelier, C. Bonnet, M. Broyer, E. Cottancin, N. Grillet, J. Lermé, J. Vialle, and M. Pellarin, *J. Phys. Chem. C* **113**, 4351 (2009).
- ⁸D. R. Ward, N. J. Halas, J. W. Ciszek, J. M. Tour, Y. Wu, P. Norlander, and D. Natelson, *Nano Lett.* **8**, 919 (2008).
- ⁹J. Tian, B. Liu, X. Li, Z. Yang, B. Ren, S. Wu, N. Tao, and Z. Tian, *J. Am. Chem. Soc.* **128**, 14748 (2006).
- ¹⁰A. Taguchi, N. Hayazawa, Y. Saito, H. Ishitobi, A. Tarun, and S. Kawata, *Opt. Express* **17**, 6515 (2009).
- ¹¹Y. Gan, *Rev. Sci. Instrum.* **78**, 081101 (2007).
- ¹²Y. Zou, P. Steinverzel, T. Yang, and K. B. Crozier, *Appl. Phys. Lett.* **94**, 171107 (2009).
- ¹³J. Colchero, A. Gil, and A. M. Baró, *Phys. Rev. B* **64**, 245403 (2001).
- ¹⁴M. Bao and H. Yang, *Sens. Actuators, A* **136**, 3 (2007).
- ¹⁵D. Sarid, J. P. Hunt, R. K. Workman, X. Yao, and C. A. Peterson, *Appl. Phys. A* **66**, 283 (1998).
- ¹⁶C. Argento and R. French, *J. Appl. Phys.* **80**, 6090 (1996).
- ¹⁷J. F. Rhoads, S. W. Shaw, and K. L. Turner, *J. Dyn. Sys., Meas., Control* **132**, 034001 (2010).
- ¹⁸N. C. Bruce, A. García-Valenzuela, and D. Kouznetsov, *J. Phys. D: Appl. Phys.* **33**, 2890 (2000).